

Fisher Pruning of Deep Nets for Facial Trait Classification

Qing Tian, Tal Arbel, James J. Clark

Centre for Intelligent Machines & ECE Department, McGill University
3480 University Street, Montreal, QC H3A 0E9, Canada

Abstract

With deep learning’s success, popular deep net structures are adopted for various vision tasks, which usually results in prohibitively high complexities for inclusion on devices without high-end GPUs. In this paper, we introduce a task-dependent neuron/filter level pruning framework based on Fisher’s LDA. The approach can be applied to convolutional, fully-connected, and module-based deep structures, in all cases leveraging the high decorrelation of neuron motifs found in the pre-decision layer and cross-layer deconv dependency. Moreover, we examine our approach’s potential in network architecture design given a specific task (e.g. facial trait classification). Experimental results on a wide array of facial traits from the LFWA and Adience datasets illustrate the framework’s superior performance to state-of-the-art pruning approaches and fixed compact structures (e.g. SqueezeNet, MobileNet). We successfully maintained comparable accuracies even after discarding most parameters (98%-99% for VGG-16, 82% for GoogLeNet) and with significant FLOP reductions (83% for VGG-16, 64% for GoogLeNet). During pruning, we could also derive smaller, but more accurate, models suitable for the task.

1. Introduction

In this paper, we explore the premise that less useful structures (including their possible redundancies) in over-parameterized deep nets can be pruned away to boost efficiency and accuracy. We argue that optimal deep features should be task dependent. In the pre-deep-learning era, features were usually hand-engineered with domain specific knowledge. Today, as a result of deep learning, we no longer need to handcraft features, but people are still handcrafting various architectures, which we believe have an impact on both the quality and quantity of features to be learned. Some features learned via suboptimal architectures may be less useful/redundant to the current task. Such features (parameters) not only add to the storage and computational burden but may also result in over-fitting when data is limited. This is especially true in transfer learning cases

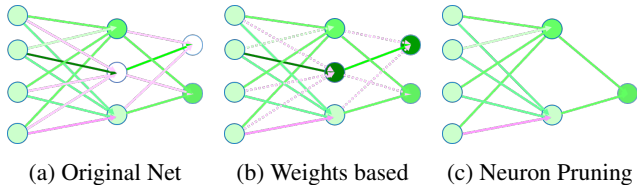


Figure 1: Weights based vs. naive activation-based neuron pruning. Green: positive, magenta: negative. Color Dark-ness indicates weight magnitude. Unlike (c), in (b), the initially dormant hidden neuron in (a) ends up firing strongly, changing the output. Dashed lines: 0 but existing weights.

where a popular ‘general’ model (e.g. ImageNet trained) is inherited and fine-tuned for the specific inference task in question (e.g. facial trait recognition).

The success of deep networks in visual classification tasks including facial trait recognition, is largely attributed to its compositionality of patterns. Moving up the layers, high-level patterns that are more complicated, global, and abstract can be built from simpler low-level patterns. In this process, the critical building block is the filter/neuron, which, through learning, is capable of capturing patterns at a certain scale of abstraction. Many pioneer pruning approaches (e.g. [13]) are based on single weight magnitudes and run the risk of destroying important patterns. For example, given a uniform input, many small negative weights may jointly counteract large positive weights and result in a dormant neuron. If pruning is based on individual weights, small negative weights would be pruned before reaching the large positive weights, engendering serious problems (e.g. Figure 1), especially when the pruning rate is high.

In this paper, we develop a neuron/filter level Fisher LDA [8] based pruning framework that is aware of both the final classification utility and its holistic dependency. This framework leads to significant space and computation savings with a possibility of boosting accuracy. Unlike previous LDA-based approaches in this direction (e.g. [50]), this paper makes several critical contributions, including: (1) the LDA measure is more accurate since it is calculated in the very last (hidden) layer where features tend

to be linearly separable (critical to LDA) and where the computed utility is directly related to the final classification. (2) the approach presented here handles a wide variety of structures such as convolutional, fully-connected, modular, and hybrid structures and prunes a full net in an end-to-end manner. It is worth noting that fully connected structures usually dominate a deep net (e.g. over 90% for both AlexNet [23] and VGG nets [44]). Previous approaches such as [50] do not prune this part. (3) we propose a novel feasible strategy to design net architectures via pruning deep modules, including determining how many filters, and of what types, are appropriate in a given layer. For example, in our age group classification experiments based on GoogLeNet, $1*1$ and $5*5$ scale filters in the Inception_5b module capture little information. They, however, are indispensable in Inception_5a. Contemporary ‘skinny’ nets such as SqueezeNet, MobileNet, and Inception nets leverage many $1*1$ filter blocks (at the module beginning/end). From our perspective, those filter blocks serve to reduce dimensionality with the number of filter blocks (new dimensions) arbitrarily set. Such ‘arbitrariness’ also exists for other filter types. Although those nets perform well for the task for which they are designed, their generalizability/adaptability to other tasks may be compromised. (4) we formulate Fisher pruning as solving a generalized eigenvalue problem and explain why it makes more sense to directly discard filters from the last hidden layer. In our experiments of recognizing facial traits (e.g. gender, smile, and age), we show how the proposed method leads to significant complexity reductions. It brings down the total VGG-16 size by 98%-99% and that of GoogLeNet by 82% without significant accuracy loss ($<1\%$). The corresponding FLOP reduction rates are about 83% and 62%, respectively. Additionally, we are able to derive more accurate models at lower complexities. In the age recognition case, one model is over 3% more accurate than the original net but only about 1/3 in size. Also, we compare our approach with some of today’s successful pruned/compact nets (e.g. MobileNet, SqueezeNet, [13], [27]) and show the importance of our proposed task dependent Fisher pruning (dimension reduction) for the facial trait classification task.

2. Related Work

2.1. Deep Neural Networks Pruning

Early approaches to artificial neural networks pruning date back to the late 1980s. Some pioneering examples include magnitude-based biased weight decay [40], Hessian based Optimal Brain Damage [25] and Optimal Brain Surgeon [14]. Since those approaches are aimed at shallow nets, assumptions that were made, such as a diagonal Hessian in [25], are not necessarily valid for deep neural networks. Please refer to [42] for more early approaches.

Over the past few years, popular deep nets have become increasingly deeper. With larger depths comes more complexity, which re-ignited research into network pruning. Han *et al.* [13] discarded weights of small magnitudes. Small weights are set to zero and masks are needed to freeze/disregard those weights during re-training. With the help of compression techniques, this sparsity is desirable for storage and transferring purposes. That said, the actual model size and computation do not change much after being deployed on general machines. Similarly, many approaches including [45, 36, 22, 10, 18, 48] sparsify networks by setting weights to zero. Unlike the above approaches, Anwar *et al.* [3] locate pruning candidates via particle filtering in a more structured way with randomly generated selection masks. More recently, neuron/filter pruning has gained popularity [39, 27, 50, 34], as they directly produce hardware friendly architectures that not only reduce the requirements of storage space and transportation bandwidth, but also bring down the initially large amount of computation in conv layers. Furthermore, with fewer intermediate feature maps generated and consumed, the number of slow and energy-consuming memory accesses is decreased, rendering the pruned nets more amenable to implementation on mobile devices. A simple yet effective approach, by Li *et al.* [27], equates filter utility to absolute weights sum. Polyak and Wolf [39] proposed a ‘channel-level’ acceleration algorithm for deep face representations based on unit variances. However, unwanted variances (e.g. lighting, pose, and makeup) and noise may be preserved or even amplified. Luo *et al.* [34] also prune on the filter level guided by the next layer’s statistics. Although impressive pruning rates have been achieved, most previous works possess one or both following drawbacks: (1) utilities are usually computed locally (relationships within layer/filter or across all layers may be missed) and (2) the utility measure is not directly related to final classification (e.g. magnitude of weights, variances, or activations).

In addition to pruning, some approaches constrain space and/or computational complexity through compression, such as Huffman encoding, weight quantization [12] and weight bitwidth reduction (e.g. XNOR-Net and BWN [41]). Some achieve space and computation savings via decompositions of filters with a low-rank assumption [6, 21, 57]. Another popular way is to adopt compact layers/modules with fewer weights (e.g. NiN [30], GoogLeNet [49], ResNet [15], SqueezeNet [20], and MobileNet [17]).

2.2. Facial Trait Classification

Facial trait classification is challenging compared to general objects, as inter-class differences of facial traits are usually subtle (e.g. telling a person’s age is more difficult than distinguishing a dog from a cat). Inner-class variances (e.g. lighting, pose, and makeup) could further complicate the

problem. Also, the recognition efficiency is critical in applications like HCI, affective computing, and interactive biometrics. Traditional approaches use global [51, 5] and/or local [1, 2, 33, 24, 46] hand-crafted features plus classic classifiers such as SVM and Bayesian QDA (alone or with some boosting algorithm). In contrast, ‘features and classifiers’ can be learned by artificial neural nets in an end-to-end manner. In the 1990s, early neural networks began to be employed for facial trait classification [9, 38, 11]. In the deep learning era, deep features and classifiers learned, generally speaking, beat handcrafted ones designed with limited domain knowledge. Verma *et al.* [53] showed the similarities between the CNN filters learned and the features that neuroscientists identified as cues utilized by humans to recognize facial traits such as gender. Levi and Hassner [26] trained and tested a not-very-deep CNN for gender and age recognition on their Adience dataset with satisfactory performance. Rather than train on images of full faces, Mansanet *et al.* [35] employed local patches to train relatively shallow nets and obtained better accuracies than full-face-image-based nets of similar depths. To make better use of shape information, Li *et al.* [28] proposed shape adaptive kernel-based tree-structured CNNs. Through pose-normalized CNNs, Zhang *et al.* [56] combined part-based models with deep nets. Liu *et al.* [31] leveraged two CNNs to detect faces and recognize facial traits sequentially, and reported satisfactory accuracies on the LFWA dataset. When labels are limited, facial features learned for identity recognition/verification (e.g. [47]) are sometimes adopted to recognize other facial traits. Finally, we propose to find optimal and compact deep face representations (net architectures/features) by task-dependent pruning. The inspiration is partly drawn from neuroscience findings [37, 52] that, despite the large number of neurons in the cerebral cortex, each neuron typically receives inputs from only a small task-dependent set of others.

3. Fisher Neuron Level Pruning for Deep Nets

In this paper, we propose a task-dependent Fisher LDA based pruning approach on the neuron/filter level that is aware of both the final classification utility and its holistic cross-layer dependency. This awareness distinguishes our pruning approach from local approaches and those with less accurate utility measures [13, 27, 39, 50]. In addition, we treat pruning as dimensionality reduction in the feature space by disentangling the factors of variation and discarding those of little utility. This is different from previously mentioned compact nets that use k 1×1 filter blocks to reduce filter/neuron level features to k dimensions (k is arbitrarily set and may be improper for a particular layer).

We begin by fully training a base deep net, using cross entropy loss with L2 regularization and Dropout that can help punish co-adaptations. We start pruning from the

last hidden layer where final classification utility is calculated. Then, the utility is traced back through deconvolution across all layers to weigh the usefulness of each neuron/filter and help decide which ones to abandon. In this way, our approach is capable of deriving optimal structures for a particular task with possible accuracy boosts.

3.1. Dimension Reduction from Last Hidden Layer

Our pruning (utility-based dimension reduction) starts from the last hidden layer because: (1) for a classification task (e.g. facial trait recognition), the utility should be the final discriminating power between the classes. Only this layer’s neurons directly and most accurately capture this discriminating power and all previous neurons feed to this layer. (2) data in this layer is more likely to be linearly separable (a key assumption of LDA while usually overlooked by many previous approaches). (3) pre-decision neuron activations representing different input patterns (motifs) are shown empirically to fire in a more decorrelated manner than earlier layers. We will see how this helps later.

We define the value of a neuron activation the neuron’s firing score (the max is taken if there are multiple across the space). Thus, for each sample image, an M -dimension firing vector can be calculated in the pre-decision layer, which we call a *firing instance* or observation ($M = 4096$ for VGG-16, $M = 1024$ for GoogLeNet). By stacking all these observations from a set of images, the firing data matrix X for that set is obtained (useless 0-variance/duplicate columns are pre-removed). Our aim here is to abandon dimensions of X that possess less discriminating power for final classification. Inspired by previous work [50, 5, 29, 4], we adopt Fisher’s LDA [8] to quantify this information utility. The goal of Fisher LDA is to maximize the class separation by finding an optimal transformation matrix W :

$$W_{opt} = \arg \max_W \frac{|W^T \Sigma_b W|}{|W^T \Sigma_w W|} \quad (1)$$

where

$$\Sigma_w = \sum_i \tilde{X}_i \tilde{X}_i^T \quad (2)$$

$$\Sigma_b = \Sigma_a - \Sigma_w \quad (3)$$

$$\Sigma_a = \tilde{X}^T \tilde{X} \quad (4)$$

with X_i being the set of observations obtained in the last hidden layer for category i . W projects the data X from its original space to a new space spanned by its columns. The tilde sign ($\tilde{\cdot}$) denotes a centering operation; for data X this means:

$$\tilde{X} = (I_n - n^{-1} \mathbf{1}_n \mathbf{1}_n^T) X \quad (5)$$

where n is the number of observations in X , $\mathbf{1}_n$ denotes an $n \times 1$ vector of ones. Finding W_{opt} involves solving a generalized eigenvalue problem:

$$\Sigma_b \vec{e}_j = v_j \Sigma_w \vec{e}_j \quad (6)$$

where (\vec{e}_j, v_j) represents a generalized eigenpair of the matrix pencil (Σ_b, Σ_w) with \vec{e}_j as a W column. If we only consider active neurons with non-duplicate patterns, we find that in the final hidden layer, most off-diagonal values in Σ_w and Σ_b are very small. In other words, besides noise/meaningless neurons, the firings of neurons representing different motifs in the pre-decision layer are highly uncorrelated. It corresponds to the intuition that, unlike common primitive features in lower layers, higher layers capture high-level abstractions of various aspects (e.g. car wheel, dog nose, flower pedals). The chances of them firing simultaneously are relatively low. In fact, different filter ‘motifs’ tend to be progressively more global and decorrelated when navigating from low to high layers. The decorrelation trend is caused by the fact that coincidences/agreements in high dimensions can hardly happen by chance. Thus, we assume that Σ_w and Σ_b tend to be diagonal in the top layer. Since inactive neurons are not considered here, Equation 6 becomes:

$$(\Sigma_w^{-1} \Sigma_b) \vec{e}_j = v_j \vec{e}_j \quad (7)$$

According to Equation 7, W columns (\vec{e}_j , where $j = 0, 1, 2, \dots, M' - 1$, $M' \leq M$) are the eigenvectors of $\Sigma_w^{-1} \Sigma_b$ (diagonal), thus they are standard basis vectors (i.e. W columns and M' of the original neuron dimensions are aligned). v_j s are the corresponding eigenvalues with:

$$v_j = \text{diag}(\Sigma_w^{-1} \Sigma_b)_j = \frac{\sigma_b^2(j)}{\sigma_w^2(j)} \quad (8)$$

where $\sigma_w^2(j)$ and $\sigma_b^2(j)$ are within-class and between-class variances along the j th neuron dimension. In other words, the optimal W columns that maximize the class separation (Eq. 1) are aligned with (a subset of) the original neuron dimensions. It turns out that when reducing dimensionality, we can directly discard dimension j s with small v_j (little contribution to Eq. 1) without much information loss.

3.2. Utility Tracing for Cross-Layer Pruning

Dimensionality reduction according to final classification utility in the pre-decision layer makes task-dependent pruning possible. The next step is to flow the utility of remaining neuron dimensions across all previous layers to guide the pruning. Unlike local approaches (focused on weights, activations, variances, ...), a pruning unit of ours cares about activation utility of filters/neurons. Higher layers, which are concerned about the contribution to final discriminability, are agnostic as how neurons are activated, in terms of the weights, input, and nonlinear rectification details. Figure 2 is an overview of our LDA-based neuron/filter level utility tracing over the layers (on a conventional CNN+FC example). The useful (cyan)

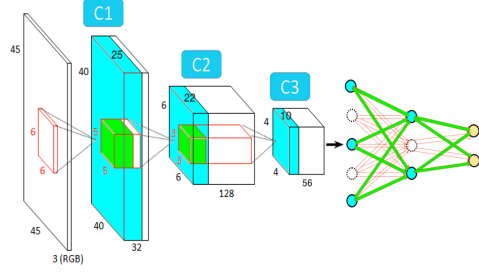


Figure 2: Overview of our full-net neuron/filter level utility tracing. Cyan indicates useful feature maps (neuron outputs/activations), green represents the corresponding parts of a next layer filter pieces (or FC weights). White denotes less relevant things to final classification.

activations (e.g. neuron outputs/feature maps) that contribute to final classification through corresponding next layer weights/filter depths (green), only depend on previous layers’ (cyan) counterparts.

We measure neuron/filter’s utility by tracing the final discriminability backwards via deconvolution (deconv) [55, 54], across all layers till the image space. The main purpose here is to reconstruct the contributing sources of useful disentangled firing patterns, instead of capturing a certain order dependency (e.g. 1st order gradient). As an inverse process of convolution (followed by nonlinear activation and pooling), our unit deconv procedure is composed of unpooling (using stored max location switches), nonlinear rectification, and reversed convolution (a transpose of the convolution Toeplitz-like matrix under an orthonormal assumption):

$$U_i = F_i^T Z_i \quad (9)$$

where i indicates the layer, the l th Z_i column is the feature vector converted from layer i feature maps w.r.t. input l , the l th U_i column is the corresponding reconstructed vector of layer i contributing sources to final utilities. On the channel level:

$$u_i^c = \frac{1}{N} \sum_{l=1}^N \sum_{j=1}^{J_i} z_{j,i,l} * f_{j,i}^{t,c} \quad (10)$$

where ‘ $*$ ’ means convolution, c indicates a channel, N is the number of training images, J is the feature map number, f^t is a deconv filter piece (determined after pre-training). It is worth noting that our calculated dependency here is data-driven and is pooled over the training set, which models the established phenomenon in neuroscience which stipulates that multiple exposures are able to strengthen relevant connections (synapses) in the brain (the Hebbian theory [16]). Here, we also extend the deconv idea to FC structures. Our idea is illustrated in Figure 3. As opposed to normal conv layers, pure FC structures can be considered as special CNNs where each neuron is a stack of $1*1$ filters

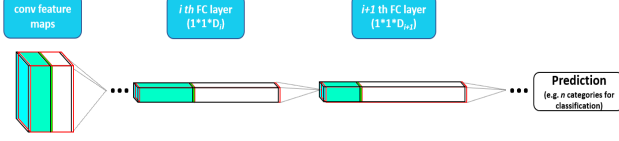


Figure 3: Diagram depicting deconv-based dependency in FC structures where a layer’s input and weights are considered as a stack of 1×1 conv feature maps and filters. The next layer’s filter and this layer’s feature maps overlap completely. There is no 1st column for pure FC structures.

with one 1×1 output feature map. Such structures do not have pooling layers in-between (or equivalently, with pooling kernels of size 1×1). As for a CNN-connected FC layer, it can also be treated as a special conv layer where the 2D convolution kernel, pooling kernel and pooling stride are of the same size as one input feature map. Instead of max pooling, the pooling layer selects the center. Thus, max switches are not necessary when unpooling for FC structures. Restructured in this way, the final utility can be successfully passed back across dense layers. For modular structures, the idea is the same except that we need to trace dependencies (apply deconvolution) for different scales in a group-wise manner. Our full net pruning, (re)training, and testing is efficient given the wide availability of end-to-end deep learning libraries.

With all neurons/filters’ utility for final discriminability known, the pruning process involves discarding structures that are less useful to final classification (e.g. structures colored white in Figures 2 and 3). When all dependencies on a neuron/filter from above layers are discarded, this neuron/filter can be abandoned. Since feature maps (neuron outputs) correspond to next-layer filter depths (neuron weights), our LDA based neuron/filter level pruning leads to both filter-wise and channel-wise savings. Mathematically speaking, input of conv layer i can be defined as one data block $B_{data,i}$ of size $d_i \times m_i \times n_i$ meaning that the input is composed of d_i feature maps of size $m_i \times n_i$ (from layer $i - 1$). Parameters of conv layer i can be considered as two blocks: the conv parameter block $B_{conv,i}$ of size $f n_i \times c n_i \times w_i \times h_i$ and the bias block $B_{bias,i}$ of size $f n_i \times 1$, where $f n_i$ is the 3D filter number of layer i , $c n_i$ is the filter depth, w_i and h_i are the width and height of a 2D filter piece in that layer. It is worth noting that $f n_{i-1} = d_i = c n_i$. $B_{conv,i}(:, k, :, :)$ operates on $B_{data,i}(k, :, :)$, which is calculated using $B_{conv,i-1}(k, :, :, :)$ (‘ $:$ ’ indicates all values along a certain dimension). When we prune away $B_{conv,i-1}(k, :, :, :)$, we effectively abandon the other two. In other words, $B_{conv,i}$ is pruned along both the first and second dimensions over the layers. When pruning, layer $i - 1$ neurons with a LDA-deconv utility score ($\max(u_i^c)$) smaller than a threshold are deleted.

Unlike many noisy and unrelated structures, the use-

ful LDA-Deconv dependencies are sparse (i.e. useful neurons/filters are at high percentiles) in most layers of a large net. This sparsity of useful dependencies is also where the room for pruning comes largely from in addition to direct reduction of neuron dimensions in the final hidden layer. To get rid of massive useless neurons quickly while be cautious in high utility regions, we set the threshold for layer i as:

$$t_i = \eta \sqrt{\frac{1}{N_i - 1} \sum_{j=1}^{N_i} (x_j - \bar{x}_i)^2} \quad (11)$$

where \bar{x}_i is the average utility of layer i activations, x_j is the utility score of the j th activation, and N_i is the total number of layer i activations (space aware). The underlying assumption is that LDA-deconv utility scores in a certain layer follow a Gaussian-like distribution. The pruning time hyper-parameter η is constant over all layers and is directly related to the pruning rate. We could set it either to squeeze the net as much as possible without obvious accuracy loss or to find the ‘most accurate’ model, or to any possible pruning rates according to the resources available and accuracies expected. In other words, rather than a fixed compact model (e.g. SqueezeNet or MobileNet), we offer the flexibility to create models customized to different needs. Adaptability is sacrificed with reduced capacity. The ‘generic’ fixed nets follow an ad-hoc direction (reducing dimensions using a ‘random’ number of 1×1 filter blocks) while our pruned models are ‘adapted’ to better fit the current task at hand (e.g. facial trait recognition). For our approach, retraining with the surviving parameters is needed after pruning.

4. Experiments and Results



Figure 4: LFWA examples (male/female, smiling/not).



(a) 0-2 (b) 4-6 (c) 8-13 (d) 15-20 (e) 25-32 (f) 38-43 (g) 48-53 (h) 60+

Figure 5: The age group examples of the Adience dataset.

In this paper, targeted at facial trait recognition, we use both conventional and module-based deep nets (i.e. VGG-16 [44] and GoogLeNet [49]) to illustrate our task-dependant pruning method. We pre-train our models on the ImageNet dataset [43], then fine-tune and test them on LFWA [31] and Adience [7] facial traits (i.e. male/female, smile/not from LFWA, and age group from Adience). These traits are chosen as examples of binary/multi-class, person specific/non-specific facial attributes. The LFWA dataset is

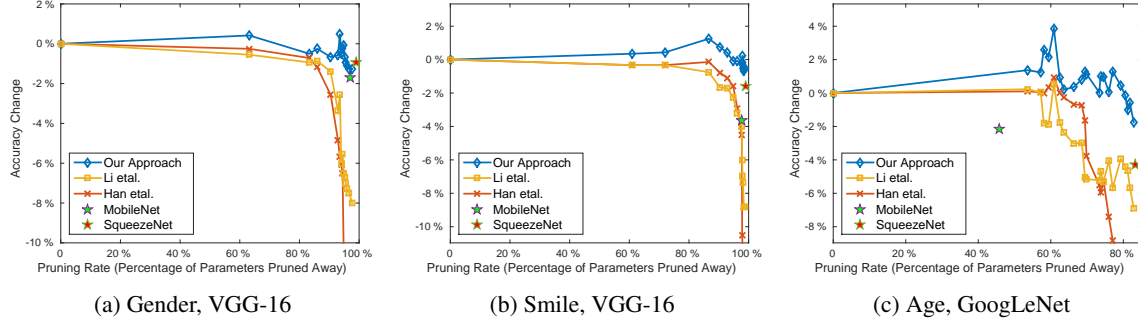


Figure 6: Accuracy change vs. parameters savings of ours (blue), Han *et al.* [13] (red), and Li *et al.* [27] (orange). For comparison, the performance of SqueezeNet [20] and MobileNet [17] have been added. The ‘parameter pruning rate’ for them implies the relative size w.r.t the original unpruned VGG-16 or GoogLeNet. In our implementation of [27], we adopt the same pruning rate as ours in each layer (rather than determine them empirically [27]).

a richly labeled version of the Labeled Faces in the Wild (LFW) database [19] and has over 13K images with 40 facial trait labels. Another dataset used is the Adience dataset, which consists of 26K images of 2,284 subjects with age group and gender labels. Both datasets cover a large range of pose and background clutter variations. The suggested splits in [31, 26] are adopted. For Adience, we use the first three folds for training, the 4th and 5th folds for validation and testing. All images are pre-resized to 224*224. Figure 4 and 5 show some example images from the two datasets.

4.1. Accuracy v.s. Pruning Rates

In this section, we analyze accuracy change v.s. complexity reductions. Figure 6 demonstrates the relationship of accuracy change with the number of parameters pruned. For comparison purposes, we add to the figures the performance of two other pruning approaches (i.e. Han *et al.* [13] and Li *et al.* [27]) as well as modern compact/pruned structures such as SqueezeNet [20] and MobileNet [17]. According to Figure 6, even with a large percentage of the parameters having been pruned away (98-99% for the VGG-16 cases, 82% for the GoogLeNet case), our approach still maintains comparable accuracy to the original models, with a loss <1%. The other two pruning approaches suffer from earlier performance degradation. This is primarily due to their utility measure. Additionally, for [13], inner filter relationships are vulnerable to pruning especially when the pruning rate is large (Figure 1). This also explains why Li *et al.* [27] performs slightly better than Han *et al.* [13] at large pruning rates. It is worth noting that during the pruning process, we come across even more accurate but lighter structures than the original net. For instance, in the age case, a model of 1/3 the original size is 3.8% more accurate than the original GoogLeNet. Similarly in the smile trait case, a 5x times smaller model can achieve 1.5% more accuracy than the unpruned VGG-16 net. That is to say, in addition to boosting efficiency, our approach provides a way to find

optimal deep models while being mindful of the resources available. Compared to the fixed compact nets (SqueezeNet and MobileNet), our pruning approach generally enjoys better performance because ‘dimensionality reduction’ in the feature space with a utility measure directly related to final classification is superior to reducing dimension using an arbitrary number of 1*1 filters. The performance differences also support our claim that pruning should be task specific. Even in the only pruning time exception where our approach has a slightly lower accuracy at the same size of SqueezeNet, much higher accuracies can be gained by simply adding back a few more parameters.

Also, we compare our approach with a previous LDA-based approach [50] where LDA is computed from intermediate conv representations. The comparison is done in terms of accuracy vs. saved computation (FLOP¹) on the VGG-16 structure (Figure 7).

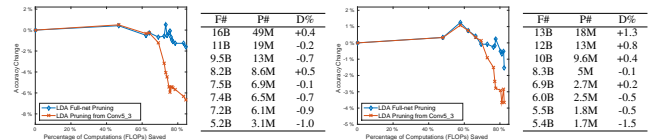


Figure 7: Accuracy change vs. FLOP savings of our approach (blue) and [50] (red) for the gender (left) and smile (right) traits on VGG-16. F# and P# are FLOPs and number of parameters, respectively. D% stands for accuracy difference with the unpruned net. Both approaches share the same F#, while the P# and D% are of our approach. FC+Softmax is used for [50].

As can be seen, the two pruning approaches perform similarly when the pruning rate is low. However, when the pruning rate increases, our pruning approach enjoys higher accuracies than [50]. The accuracy difference can be as large as 6% (on validation data). The reason is that our LDA utility is more accurate, as it is computed where the

¹As in [13], both multiplication and addition account for 1 FLOP.

Table 1: Testing accuracies. ‘AF’ and ‘PF’ represents accuracy first and param# first strategies when selecting models. Our approach’s param# and FLOPs (last row) are respectively shared by [27, 13] and [27, 50]. [13] has the same FLOPs as the base models. The base models’ testing accuracies are included in the first row parentheses. Original param# and FLOPs for VGG-16, GoogLeNet, MobileNet, and SqueezeNet are 138M, 6.0M, 4.3M, 1.3M and 31B, 3.2B, 1.1B, 1.7B, respectively.

| Methods & Acc | Gender (VGG, 91%) | | Smile (VGG, 91%) | | Age (GoogLeNet, 55%) | |
|-------------------------|-------------------|-------------|------------------|-------------|----------------------|-------------|
| | AF | PF | AF | PF | AF | PF |
| MobileNet [17] | 89% | | 87% | | 49% | |
| SqueezeNet [20] | 90% | | 88% | | 50% | |
| Han <i>et al.</i> [13] | 89% | 83% | 91% | 81% | 56% | 43% |
| Li <i>et al.</i> [27] | 88% | 85% | 91% | 83% | 56% | 46% |
| Tian <i>et al.</i> [50] | 90% | 88% | 92% | 88% | 58% | 54% |
| Our approach | 93% | 92% | 93% | 90% | 58% | 54% |
| (Param#,FLOP) | (6.5M,7.4B) | (3.1M,5.2B) | (18M,13B) | (1.8M,5.5B) | (2.3M,1.8B) | (1.1M,1.1B) |

linear assumption of LDA is more likely to be met and where the utility is directly related to final classification.

To assess generalization ability on unseen data, in Table 1, we select our model with the highest accuracy (accuracy first strategy) and the lightest one with less than 1% accuracy loss (param# first strategy) on the validation data for each task, and report accuracies on the test sets. The competing approaches are also included. From Table 1, it is evident that our approach generalizes well to unseen data (highest accuracies over most cases). Its superiority is more obvious in the ‘param# first’ case. This agrees with previous validation results. Additionally, the accuracy gaps between the fixed nets and our pruning approach become larger than on validation data because arbitrary and task independent way of ‘selecting’ filter dimensions constrained nets’ generalizability to unseen images for the current task. Finally, our approach performs even better on the GoogLeNet than on the VGG-16s as the former gives our method the flexibility to select both filter types/sizes and filter numbers.

4.2. Layerwise Complexity Analysis

In this section, we provide a layer-by-layer complexity analysis of our pruned nets in terms of parameters and computation. The net we select for each case is the one that preserves similar classification power (loss within 1%) to the original net, but with as few parameters as possible. Figure 8, 9, 10 demonstrate layer-wise complexity reductions of the gender, smile/no smile, and age cases respectively. The base structure for the former two is VGG-16, and the one in the age case is GoogLeNet. Since parameters in fully connected layers dominate the whole VGG-16 net, we add a separate layer-wise parameter analysis for conv layers in the two VGG-16 cases. From these results, it is evident that our approach has led to significant parameter and FLOP reductions across the layers. Particularly, the reduction in parameters for the VGG-16 models mainly come from the first FC layer (i.e. FC6) due to the fact that the last conv layer output (after pooling) still has so many ‘pixels’ that,

when fully connected with first FC layer’s neurons (4096 in VGG-16), they generate a huge number of parameters. On the contrary, the total conv parameter number has nothing to do with input feature map (2D) dimension due to the weight sharing scheme. We can also see that higher layers, in general, have higher parameter pruning rates than the first three layers. This makes sense as earlier layers correspond to primitive patterns (e.g. edges, corners, and color blobs) that are commonly useful. Figure 10 shows the case of classifying age with the GoogLeNet as the base model. In each Inception module, different kinds of filters are pruned differently. For example, from right, the 2nd-4th modules prefer 1*1 and 5*5 filters more than other modules do. 3*3 filters are more desirable than other types in Inception_3b, 4d and 4e (abundant information lies on the 3*3 scale in those modules). In pruned Inception_5b, 3*3 is the only filter type left (not considering the preceding 1*1 filters). As we can see, our approach provides a way to design deep architecture by choosing the kinds of filters and also the filter number for each kind. In our pruned models (pruned VGG-16 and GoogLeNet), most parameters in the middle layers have been discarded. Those remaining filters can possibly be collapsed to reduce net depth. For instance, most or all filters left in the middle modules in Figure 10 are of size 1*1. They can be viewed as filter selectors (by weight assignment) and thus can be combined (and maybe merged into the previous module concatenation to form a weighted summation). Such ‘skipping’ modules pass feature representations to higher layers without (much) increment of the features’ level of abstraction. In addition to the GoogLeNet (Inception V1) example, our approach can prune other modular structures, such as ResNet where the final summation in a unit module can be modeled as a concatenation followed by convolution. In terms of storage, our pruned nets are light. On a machine with 32-bit parameters the above models are respectively 12MB, 6.9MB, and 4.3MB. Those light models can possibly fit into computer/cellphone memories or even caches (with super-linear efficiency boosts).

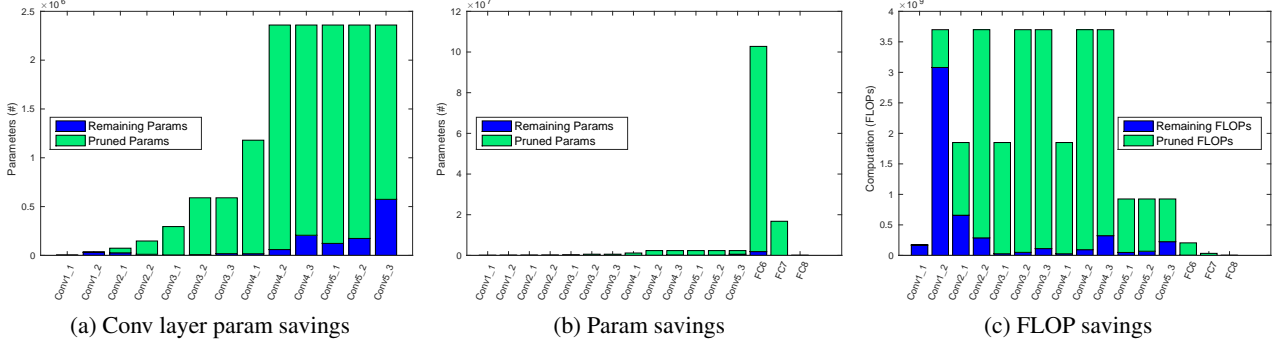


Figure 8: Layerwise complexity reductions (gender, VGG16).

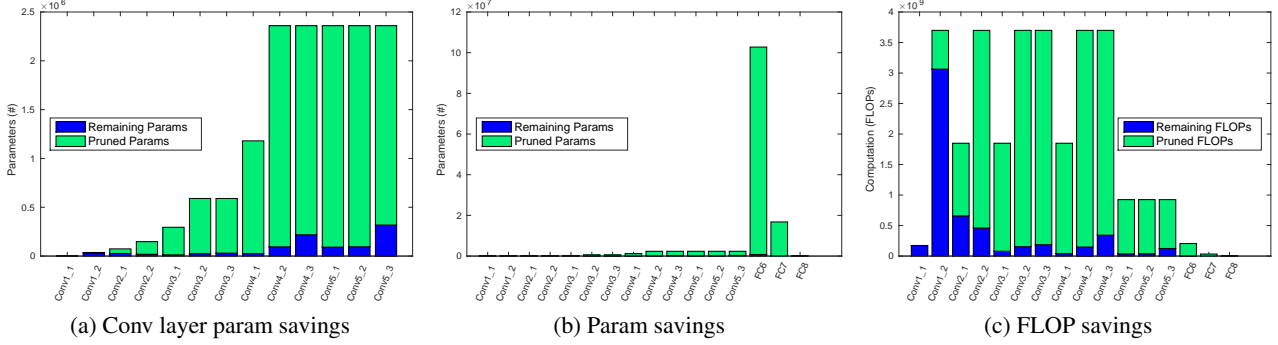


Figure 9: Layerwise complexity reductions (smile, VGG16).

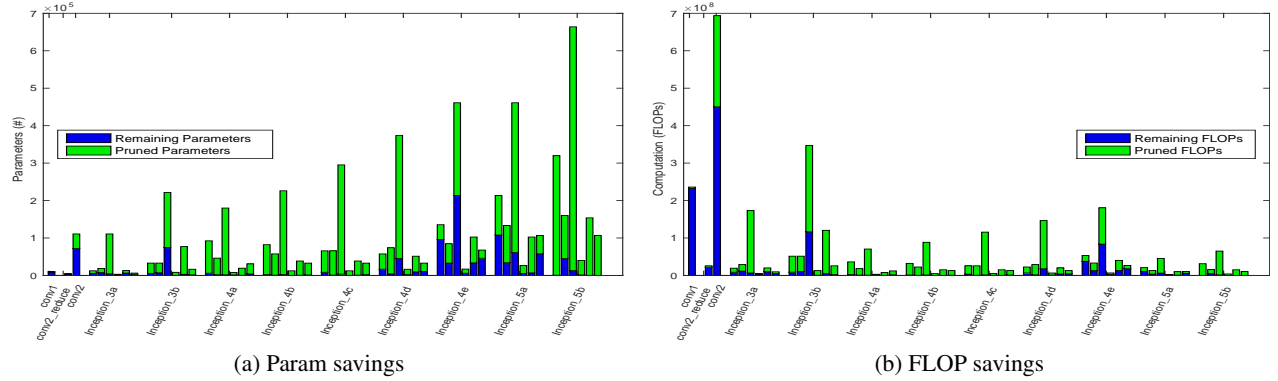


Figure 10: Layerwise complexity reductions (age, GoogLeNet). From left to right, the conv layers in a Inception module are (1*1), (1*1,3*3), (1*1,5*5), (1*1 after pooling).

5. Conclusion

In this paper, we have proposed a task-dependent neuron level end-to-end pruning approach with a LDA-Deconv utility that is aware of both final classification and its holistic cross-layer dependency. This is different from previous approaches with an indirect (usually less accurate) and/or local (individual weight or within 1-2 layers) utility measure. Our approach is able to prune convolutional, fully connected, modular, and hybrid deep structures and it provides a practical way to deep model design by finding both the desired types of filters as well as the number for each

kind. Compared to fixed nets with sacrificed adaptability, we offer a range of models (trade-offs between accuracy and efficiency) that are suitable for the current task at hand. In facial trait classification on LFWA and Adience examples, our approach achieves greater complexity reductions than competing methods (over 98% of VGG-16, 82% of GoogLeNet parameters as well as 83% of VGG-16, 64% of GoogLeNet computations have been saved without obvious accuracy loss). The great pruning rates and structured nature of the approach offers great potential for installation on mobile devices without powerful GPUs.

References

- [1] T. Ahonen, A. Hadid, and M. Pietikäinen. Face recognition with local binary patterns. In *European conference on computer vision*, pages 469–481. Springer, 2004. 3
- [2] T. Ahonen, A. Hadid, and M. Pietikäinen. Face description with local binary patterns: Application to face recognition. *IEEE transactions on pattern analysis and machine intelligence*, 28(12):2037–2041, 2006. 3
- [3] S. Anwar, K. Hwang, and W. Sung. Structured pruning of deep convolutional neural networks. *arXiv preprint arXiv:1512.08571*, 2015. 2
- [4] J. Bekios-Calfa, J. M. Buenaposada, and L. Baumela. Revisiting linear discriminant techniques in gender recognition. *IEEE Transactions on Pattern Analysis and Machine Intelligence*, 33(4):858–864, 2011. 3
- [5] P. N. Belhumeur, J. P. Hespanha, and D. J. Kriegman. Eigenfaces vs. fisherfaces: Recognition using class specific linear projection. *IEEE Transactions on pattern analysis and machine intelligence*, 19(7):711–720, 1997. 3
- [6] E. L. Denton, W. Zaremba, J. Bruna, Y. LeCun, and R. Fergus. Exploiting linear structure within convolutional networks for efficient evaluation. In *Advances in neural information processing systems*, pages 1269–1277, 2014. 2
- [7] E. Eidinger, R. Enbar, and T. Hassner. Age and gender estimation of unfiltered faces. *IEEE Transactions on Information Forensics and Security*, 9(12):2170–2179, 2014. 5
- [8] R. A. Fisher. The use of multiple measurements in taxonomic problems. *Annals of eugenics*, 7(2):179–188, 1936. 1, 3
- [9] B. A. Golomb, D. T. Lawrence, and T. J. Sejnowski. Sexnet: A neural network identifies sex from human faces. In *NIPS*, volume 1, page 2, 1990. 3
- [10] Y. Guo, A. Yao, and Y. Chen. Dynamic network surgery for efficient dnns. In *Advances In Neural Information Processing Systems*, pages 1379–1387, 2016. 2
- [11] S. Gutta and H. Wechsler. Gender and ethnic classification of human faces using hybrid classifiers. In *Neural Networks, 1999. IJCNN’99. International Joint Conference on*, volume 6, pages 4084–4089. IEEE, 1999. 3
- [12] S. Han, H. Mao, and W. J. Dally. Deep compression: Compressing deep neural network with pruning, trained quantization and huffman coding. *CoRR, abs/1510.00149*, 2, 2015. 2
- [13] S. Han, J. Pool, J. Tran, and W. Dally. Learning both weights and connections for efficient neural network. In *Advances in Neural Information Processing Systems*, pages 1135–1143, 2015. 1, 2, 3, 6, 7
- [14] B. Hassibi and D. G. Stork. *Second order derivatives for network pruning: Optimal brain surgeon*. Morgan Kaufmann, 1993. 2
- [15] K. He, X. Zhang, S. Ren, and J. Sun. Deep residual learning for image recognition. In *Proceedings of the IEEE conference on computer vision and pattern recognition*, pages 770–778, 2016. 2
- [16] D. O. Hebb. *The organization of behavior: A neuropsychological theory*. Psychology Press, 2005. 4
- [17] A. G. Howard, M. Zhu, B. Chen, D. Kalenichenko, W. Wang, T. Weyand, M. Andreetto, and H. Adam. Mobilenets: Efficient convolutional neural networks for mobile vision applications. *arXiv preprint arXiv:1704.04861*, 2017. 2, 6, 7
- [18] H. Hu, R. Peng, Y.-W. Tai, and C.-K. Tang. Network trimming: A data-driven neuron pruning approach towards efficient deep architectures. *arXiv preprint arXiv:1607.03250*, 2016. 2
- [19] G. B. Huang, M. Ramesh, T. Berg, and E. Learned-Miller. Labeled faces in the wild: A database for studying face recognition in unconstrained environments. Technical Report 07-49, University of Massachusetts, Amherst, October 2007. 6
- [20] F. N. Iandola, S. Han, M. W. Moskewicz, K. Ashraf, W. J. Dally, and K. Keutzer. Squeezenet: Alexnet-level accuracy with 50x fewer parameters and <0.5 mb model size. *arXiv preprint arXiv:1602.07360*, 2016. 2, 6, 7
- [21] M. Jaderberg, A. Vedaldi, and A. Zisserman. Speeding up convolutional neural networks with low rank expansions. *arXiv preprint arXiv:1405.3866*, 2014. 2
- [22] X. Jin, X. Yuan, J. Feng, and S. Yan. Training skinny deep neural networks with iterative hard thresholding methods. *arXiv preprint arXiv:1607.05423*, 2016. 2
- [23] A. Krizhevsky, I. Sutskever, and G. E. Hinton. Imagenet classification with deep convolutional neural networks. In *Advances in neural information processing systems*, pages 1097–1105, 2012. 2
- [24] N. Kumar, A. C. Berg, P. N. Belhumeur, and S. K. Nayar. Attribute and simile classifiers for face verification. In *Computer Vision, 2009 IEEE 12th International Conference on*, pages 365–372. IEEE, 2009. 3
- [25] Y. LeCun, J. S. Denker, S. A.olla, R. E. Howard, and L. D. Jackel. Optimal brain damage. In *NIPs*, volume 2, pages 598–605, 1989. 2
- [26] G. Levi and T. Hassner. Age and gender classification using convolutional neural networks. In *Proceedings of the IEEE Conference on Computer Vision and Pattern Recognition Workshops*, pages 34–42, 2015. 3, 6
- [27] H. Li, A. Kadav, I. Durdanovic, H. Samet, and H. P. Graf. Pruning filters for efficient convnets. *arXiv preprint arXiv:1608.08710*, 2016. 2, 3, 6, 7
- [28] S. Li, J. Xing, Z. Niu, S. Shan, and S. Yan. Shape driven kernel adaptation in convolutional neural network for robust facial traits recognition. In *Proceedings of the IEEE Conference on Computer Vision and Pattern Recognition*, pages 222–230, 2015. 3
- [29] Y. Li, J. Kittler, and J. Matas. Effective implementation of linear discriminant analysis for face recognition and verification. In *Computer Analysis of Images and Patterns*, page 234. Springer, 1999. 3
- [30] M. Lin, Q. Chen, and S. Yan. Network in network. *ICLR*, 2014. 2
- [31] Z. Liu, P. Luo, X. Wang, and X. Tang. Deep learning face attributes in the wild. In *Proceedings of International Conference on Computer Vision (ICCV)*, December 2015. 3, 5, 6

- [32] J. Long, E. Shelhamer, and T. Darrell. Fully convolutional networks for semantic segmentation. In *Proceedings of the IEEE Conference on Computer Vision and Pattern Recognition*, pages 3431–3440, 2015.
- [33] D. G. Lowe. Object recognition from local scale-invariant features. In *Computer vision, 1999. The proceedings of the seventh IEEE international conference on*, volume 2, pages 1150–1157. Ieee, 1999. 3
- [34] J.-H. Luo, J. Wu, and W. Lin. Thinet: A filter level pruning method for deep neural network compression. In *Proceedings of the IEEE international conference on computer vision*, pages 5058–5066, 2017. 2
- [35] J. Mansanet, A. Albiol, and R. Paredes. Local deep neural networks for gender recognition. *Pattern Recognition Letters*, 70:80–86, 2016. 3
- [36] Z. Mariet and S. Sra. Diversity networks. *ICLR*, 2016. 2
- [37] V. B. Mountcastle et al. Modality and topographic properties of single neurons of cats somatic sensory cortex. *J neurophysiol*, 20(4):408–434, 1957. 3
- [38] B. Poggio, R. Brunelli, and T. Poggio. Hyperbolic networks for gender classification. 1992. 3
- [39] A. Polyak and L. Wolf. Channel-level acceleration of deep face representations. *IEEE Access*, 3:2163–2175, 2015. 2, 3
- [40] L. Y. Pratt. *Comparing biases for minimal network construction with back-propagation*, volume 1. Morgan Kaufmann Pub, 1989. 2
- [41] M. Rastegari, V. Ordonez, J. Redmon, and A. Farhadi. Xnor-net: Imagenet classification using binary convolutional neural networks. In *European Conference on Computer Vision*, pages 525–542. Springer, 2016. 2
- [42] R. Reed. Pruning algorithms—a survey. *IEEE transactions on Neural Networks*, 4(5):740–747, 1993. 2
- [43] R. Rothe, R. Timofte, and L. V. Gool. Deep expectation of real and apparent age from a single image without facial landmarks. *International Journal of Computer Vision (IJCV)*, July 2016. 5
- [44] K. Simonyan and A. Zisserman. Very deep convolutional networks for large-scale image recognition. In *Proceedings of the International Conference on Learning Representations (ICLR) 2015*, 2015. 2, 5
- [45] S. Srinivas and R. V. Babu. Data-free parameter pruning for deep neural networks. *arXiv preprint arXiv:1507.06149*, 2015. 2
- [46] V. Štruc and N. Pavešić. Gabor-based kernel partial-least-squares discrimination features for face recognition. *Informatica*, 20(1):115–138, 2009. 3
- [47] Y. Sun, X. Wang, and X. Tang. Deeply learned face representations are sparse, selective, and robust. In *Proceedings of the IEEE Conference on Computer Vision and Pattern Recognition*, pages 2892–2900, 2015. 3
- [48] V. Sze, T.-J. Yang, and Y.-H. Chen. Designing energy-efficient convolutional neural networks using energy-aware pruning. pages 5687–5695. 2
- [49] C. Szegedy, W. Liu, Y. Jia, P. Sermanet, S. Reed, D. Anguelov, D. Erhan, V. Vanhoucke, and A. Rabinovich. Going deeper with convolutions. In *Proceedings of the IEEE Conference on Computer Vision and Pattern Recognition*, pages 1–9, 2015. 2, 5
- [50] Q. Tian, T. Arbel, and J. J. Clark. Deep lda-pruned nets for efficient facial gender classification. In *Computer Vision and Pattern Recognition Workshops (CVPR Workshop on Biometrics), 2017 IEEE Conference on*, pages 512–521. IEEE, 2017. 1, 2, 3, 6, 7
- [51] M. A. Turk and A. P. Pentland. Face recognition using eigenfaces. In *Computer Vision and Pattern Recognition, 1991. Proceedings CVPR’91., IEEE Computer Society Conference on*, pages 586–591. IEEE, 1991. 3
- [52] L. G. Valiant. A quantitative theory of neural computation. *Biological cybernetics*, 95(3):205–211, 2006. 3
- [53] A. Verma and L. Vig. Using convolutional neural networks to discover cognitively validated features for gender classification. In *Soft Computing and Machine Intelligence (ISCMi), 2014 International Conference on*, pages 33–37. IEEE, 2014. 3
- [54] M. D. Zeiler and R. Fergus. Visualizing and understanding convolutional networks. In *European Conference on Computer Vision*, pages 818–833. Springer, 2014. 4
- [55] M. D. Zeiler, G. W. Taylor, and R. Fergus. Adaptive deconvolutional networks for mid and high level feature learning. In *2011 International Conference on Computer Vision*, pages 2018–2025. IEEE, 2011. 4
- [56] N. Zhang, M. Paluri, M. Ranzato, T. Darrell, and L. Bourdev. Panda: Pose aligned networks for deep attribute modeling. In *Proceedings of the IEEE Conference on Computer Vision and Pattern Recognition*, pages 1637–1644, 2014. 3
- [57] X. Zhang, J. Zou, K. He, and J. Sun. Accelerating very deep convolutional networks for classification and detection. *IEEE transactions on pattern analysis and machine intelligence*, 38(10):1943–1955, 2016. 2